2020 IEEE International Conference on Robotics and Automation (ICRA)
31 May - 31 August, 2020. Paris, France

A Compact and Low-cost Robotic Manipulator Driven by Supercoiled Polymer Actuators

Yang Yang[1,2,*], *Member, IEEE,* Zhicheng Liu[2], Yanhan Wang[2], Shuai Liu[2], and Michael Yu Wang[2,3], *Fellow, IEEE*

***Abstract*— The supercoiled polymer (SCP) actuator is a novel artificial muscle, which is manufactured by twisting and coiling polymer fibers. This new artificial muscle is soft, low-cost and shows good linearity. Being utilized as an actuator, the artificial muscle could generate significant mechanical power in a muscle-like form upon electrical activation by Joule heating. In this study, we adopt this new artificial muscle to actuate a novel designed robotic manipulator, which is composed of two parts. The first part is a robotic arm based on the inspiration of the musculoskeletal system. The arm is fabricated with two ball-and-socket joints as skeleton and SCP actuators as driven muscles. The second part is a Fin Ray Effect inspired soft gripper that can perform grasping tasks on fragile objects. The manipulator prototype is fabricated and experimental tests are conducted including both simple but effective control of the bio-inspired arm as well as characterization of the gripper. Lastly, a pick and place demonstration of a fragile fruit is performed utilizing the proposed manipulator. We envision that the bio-inspired robotic manipulator design driven by SCP actuators could potentially be used in other robotic applications.**

I. INTRODUCTION

The musculoskeletal system (MS) is a significant biological system, which enables humans and other animals to perform different and complex movements based on the contraction of muscles. Various robotic applications based on MS have been built, such as robotic arm [1], robotic hand [2], legged locomotion [3], etc. Biomimetic robots inspired by MS mostly rely on electric motors for actuation. Though they can provide enough force and accurate positioning, electric motors have some disadvantages for robots based on the musculoskeletal system [4]. Electric motors usually require complex gear systems, which leads to bulky structure and large volume [5, 6]. Many of the common designs are building on a high-torque servo motor and a low backlash reduction gear. These classical designs tend to be relatively expensive, heavy, and bulky. Particularly, high ratio reduction gears have been a major limitation to low-cost robot designs. Thus, electric motors are not fit for the bio-inspired design, which means that a muscle-like actuator is required to build a compact bio-inspired robotic system.

Research is supported by the Startup Foundation for Introducing Talent of NUIST, and the Hong Kong Innovation and Technology Fund (ITF) ITS-018-17FP.

[1]School of Automation, Nanjing University of Information Science and Technology, Nanjing 210044, China

[2]Department of Mechanical and Aerospace Engineering, Hong Kong University of Science and Technology, Hong Kong.

[3]Department of Electronic and Computer Engineering, Hong Kong University of Science and Technology, Hong Kong.

*Corresponding author. Tel:+852-67264174, meyang@nuist.edu.cn

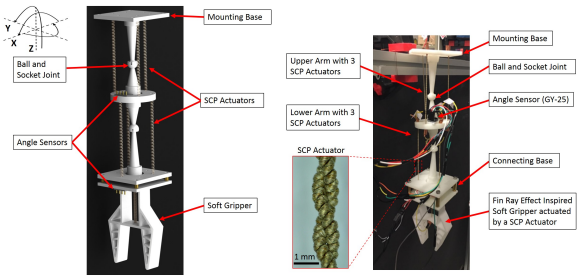

Fig. 1: Proposed robotic manipulator. (a) 3D model. (b) Real prototype.

Biological muscle tissue is often used as a standard reference of performance to develop novel robotic actuators [7]. Biological muscles have excellent capabilities, including high power-to-weight ratio, high dynamic range, making them unique and ideal actuators. Inspired by biological muscles, scientists have developed many artificial muscles that present the desirable properties of biological muscles. Among existing artificial muscles, the common ones include pneumatic artificial muscles (PAMs) [8], shape memory alloy (SMA) actuators [9], dielectric elastomer actuators (DEAs) [10], ionic polymer-metal composites (IPMC) actuators [11], supercoiled polymer (SCP) actuators [12] and so on.

Among the pneumatic artificial muscles, the most commonly used are McKibben actuators, which pressurize and decompress the sheath for contraction and relaxation, providing high output power and behave like skeletal muscles [8]. Whereas, for the pneumatic actuators, an air compressor is required to force gas into the actuator to create a difference in pressure for actuation between the interior and the surrounding environment, which also leads to bulky structure and large volume.

Shape memory alloy (SMA) materials often use these generator systems: electrical activation, photoactivation, and chemical activation. This result, respectively, in cross-sectional shrinking and expansion of the material during activation and deactivation. Regardless of the configuration, SMA relies on martensite versus austenite transformation, creating a giant hysteresis throughout activation, limiting its controllability. Moreover, the recoverable strain of the SMA wire is in the range of 4% to 8%, which is relatively small [9].

Recently, a new type of actuator called SCP artificial muscle has been discovered by Haines et al [12]. It was built by continually twisting polymer threads, and it would

form a coiled structure. Large tensile actuation (strain) is produced by the actuator. According to the experiments of Haines, SCP could provide tensile actuation with high load-carrying capability. Also, it could be actuated by Joule heating, which means it is conveniently controlled by changing the current through the conductive coating surface of the polymer, thus, it could be implemented simply based on a thermomechanical property. Compared to the first two actuators, SCP has notable advantages in various aspects. It is easily manufactured by commercial nylon fibers such as nylon threads or fishing lines. Thus, to fabricate the actuator is relatively low cost. According to the experimental data, SCP has an ideal linear property, which could make help to design a control system [13].

Unlike the existing cable-driven robot design used the classical motor actuator [6], our design used the SCP actuators. To actuate a ball joint in [6], three motors and capstans are needed, making the whole structure bulky and the cost is much higher than using the SCP actuators. In contrast, the design in this study is light and the whole structure is compact. A further difference with motor & cable driven design is that SCP generates distributed force along its whole length while force is transferred from one end to another in motor & cable driven robot. As for the pneumatic artificial muscle driven robotic arm, affiliated devices such as air compressors and valves are also indispensable, making the whole robotic system less compact. SMA actuated robotic system is also compact and large stress can be generated. However, SMA actuators usually suffer from limited controllability due to substantial hysteresis during the phase transition. In summary, the existing actuation approaches for continuum and hyper-redundant robotic arm all have their advantages and disadvantages, which calls out the need for novel actuation technologies. In this research, we adopt the SCP actuators for driving both a bio-inspired robotic arm and also a soft gripper.

A variety of robotic applications have been reported using the SCP actuators such as humanoid robotic hand [14], wrist orthosis [15], inchworm-inspired robot [16], shape-morphing structure [17] and soft finger [18]. However, many aspects of the SCP actuation system are still under investigation, including the design, sensing and control [19]. The research of SCP is still an underexplored area. Wu et al. have investigated the application of SCP actuators in the musculoskeletal system recently [20]. They focused on the characterization of SCP muscle with a new fabrication approach and experimental tests of the single joint musculoskeletal system. Different from their research, in this study, a single joint musculoskeletal system serves as the basic block for building a robotic arm. Both open loop control based on modeling and closed loop control with sensory feedback are investigated. Moreover, we also designed a compact Fin Ray Effect inspired soft gripper as an end effector assembled to the robot arm to perform grasping tasks.

The Fin Ray Effect was discovered by biologist Leif Kniese of Evologics and is based on the deformation of the fish fins [21]. The fingers of the gripper can automatically wrap around the object in spite of their shapes. And due to the soft material used, the gripper can grasp fragile objects. The gripper is actuated by a single SCP actuator, thus it has a simple structure and easy controllability.

The assembly of the proposed robotic manipulator is illustrated in Fig. 1. Each SCP actuator is driven independently. The major contributions of this study include:

- Novel design of a compact and low cost robotic manipulator driven by SCP actuators;
- Simple open loop and closed loop control of SCP powered robotic arm;
- Compact Fin Ray Effect inspired soft-material gripper powered by SCP for handling fragile and irregular objects.

The rest of this paper is organized as follows. Section II presents the design of the robotic manipulator prototype. The fabrication and assembly of the whole robotic system are given in Section III. Then, the open loop and closed loop control of the robotic arm and the characterization of soft gripper are given in Section IV. Grasping demonstration using the proposed robotic manipulator is also presented in this section. Lastly, Section V concludes the paper and discusses future work.

II. DESIGN OF THE ROBOTIC MANIPULATOR

A. Robotic arm

The characteristics of SCP actuators are desirable and well matched to the needs of artificial muscles. These include linear output, simple control, and factor of slender shape. SCP actuators enjoy considerable controllability advantages over SMA actuators, where SMAs rely on phase transitions from martensite to austenite. Based on the characteristics of SCP actuators, we designed a bio-inspired arm, where SCP actuators serve as muscles and the ball-and-socket joint serves as the skeletal system of the robotic arm. Based on the ball-and-socket joint, we built the robotic arm by cascading two of these joints. The novelty of this motor-free robotic arm design is the absence of the space occupying motor and the motor holder, contributing to the system compactness and possible applications in limited spaces where traditional motors and pumps can not be used. In future, we can enrich the motion and improve the workspace of the manipulator by cascading more ball joints in the robotic arm (as elephant truck type).

As shown in Fig. 1(a), the proposed robotic arm has two joints and SCP muscles have been used as contraction actuators driving the ball-and-socket joint to provide multidimensional motions. However, the degree of freedom (DOF) of the robotic arm depends on the way to install the SCP actuators. For the current configuration (Fig. 1(a)), 3 SCP muscles of equal length were placed in each joint with an equal angle interval (120°). The SCP muscles are in parallel with the Z axis in the primary state, which makes the joint rotating about X and Y axis. Thus, the robotic arm would have 4 DOFs. If the SCP actuators are installed inclined, it could provide rotation about Z axis, thus the arm has 6 DOFs in total.

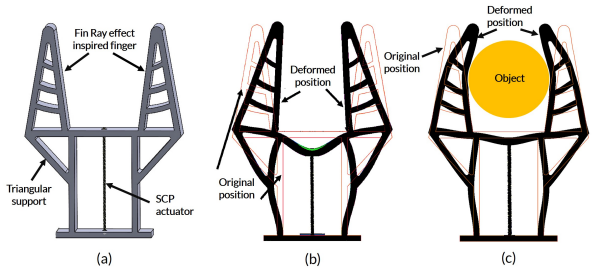

Fig. 2: Soft gripper design. (a) 3D model of Fin Ray effect inspired soft gripper. (b) Gripper free deformation upon SCP actuation without grasped object. (c) Gripper deformation upon SCP actuation with grasped object.

The MS structure relies on the contraction of artificial muscles to pull the skeleton for versatile movements. Each actuator could be controlled independently to produce angular displacement of the joint. And to actuate two adjacent actuators in each link could provide angular displacement along the middle direction. As for the recuperative procedure, as the actuated muscle contracts, the other unactuated actuators extend due to the moving of the arm and thereby store energy to accelerate the recovery procedure. To further decrease the recovering time, unactuated actuator could be actuated during the recuperative process. The positioning and orientation of the end-effector are controlled by changing the lengths of the six linear SCP actuators which are fixed on the base and joint platform.

B. Novel Fin Ray Effect inspired soft gripper

The traditional Fin Ray Effect module comprises a V-shape wall structure and parallel rib structure inside the wall structure. When a force is applied to the wall structure, the structure tends to bend to envelop the force. Thus, the Fin Ray Effect inspired gripper can adjust itself to the shape of the object to be grasped [22]. Compared to traditional parallel ribs structure, Bason has proved that when the ribs were slanted and curved, the Fin Ray Effect structure had 29.3% lager deformation [23].

Based on previous studies, we designed a Fin Ray Effect inspired gripper which is actuated by a single SCP actuator, the design is showed in Fig. 2(a). When the SCP is activated by Joule heating, the two fingers of the gripper tend to close as illustrated in Fig. 2(b). When encountered with the grasped object, the Fin Ray Effect will operate and the fingers will conform around the object to realize firm grasping as shown in Fig. 2(c). The gripper is fabricated by soft material so that it can handle fragile objects safely benefited from its inherent compliance. The novelty of this gripper design is that using a SCP actuator to actuate the fin-ray gripper makes the whole structure lightweight and compact. Compared to the gripper in [22], a motor holder together with the motor and pulley are no longer needed, which also makes it possible for miniaturization of the gripper for applications such as in minimally invasive surgery. As an end effector attached to the robotic arm, the reduced weight contributed by this novel gripper would improve the load carrying capability of the whole robotic manipulator.

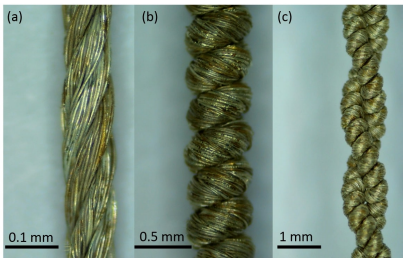

Fig. 3: Micrographs. (a) Nylon fishing line. (b) One-ply coiled SCP actuator. (c) Two-ply coiled SCP actuator used in this study.

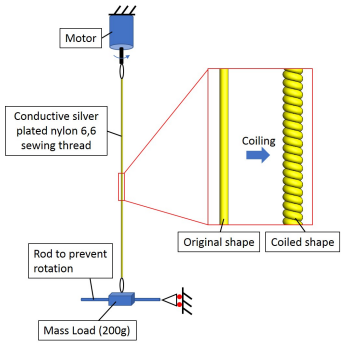

Fig. 4: SCP artificial muscle fabrication setup.

III. FABRICATION AND ASSEMBLY

A. Fabrication of SCP actuator

The artificial muscles are made of twisted and coiled polymer thread for our musculoskeletal robot. Material selection and ways to manufacture play important roles in the performance of the SCP actuator. SCP could be made with fishing line and sewing threads made of nylon, polyethylene or other materials [12]. In our design, we used the conductive silver coated nylon thread, because it does not require a complicated manufacturing process. It could avoid twisting or warping a very thin resistance wire, which is hard and easy to break during the fabrication procedure of the polymer. The thread used in this study is conductive Silver Plated Nylon 6,6 sewing thread manufactured by Shieldex Trading, Inc (part number: 700000301091), which is shown in Fig. 3(a).

The thread used a 200g load, which should keep the thread taut and straight while being twisted, because it may twine during the coil-forming if the load could not keep the fiber tight, also it should not be too heavy to make the thread snap during the process. The setup of fabrication is shown as Fig. 4. At a certain point, the twisting of the thread will begin to form one-ply coils along its length (Fig. 3(b)). When the thread is completely coiled, it is double-backed on itself to create a two-ply polymer. This prevents the coils from unwinding, just as Fig. 3(c) shows.

After the initial procedure, the SCP could not behave well, as a precursor, we could find that it is curly in a natural state and could only perform few strokes. Thus, coiled fiber needs electrothermal annealing and training to strengthen performance. A large load (400 g) is used during the annealing process. A square voltage of 17 V pulse of 2.5 seconds on and then 20 seconds off was applied 5 times at

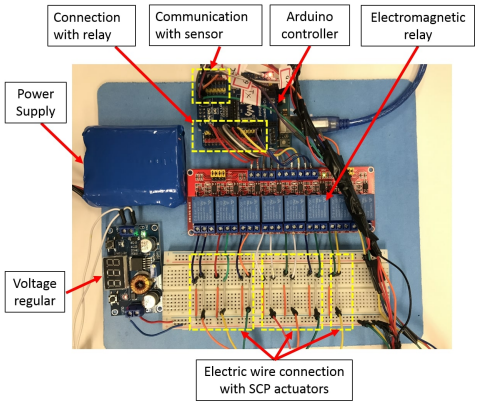

Fig. 5: Control board of the robotic manipulator.

first, then one cycle of 5 seconds voltage on was applied following 50 seconds rest time. This way could heat the coiled fiber rapidly and then provide enough time for cooling and elongation before the next cycle. Upon further applying cyclic voltage, the length of the coiled fiber would achieve a maximum strain. Then, we replaced the 400 g mass load with a 100 g mass to continue the annealing training, to eliminate the effect of over elongation of the heavy mass load. At last, we tested it with a cyclic voltage pulse 8 V (20 s on and 50 s off) with 100 g load, and it could be observed that the displacement is stable. This could be seen as the final stable state. Further details with regard to the fabrication process of SCP actuators can be found in [24, 25]. Performance parameters of the fabricated SCP actuator (105 mm length) are: maximal stroke of 15%, weight of 0.26 g (without electrode) and electrical resistance of 0.05 Ω/mm.

B. Assembly of the proposed robotic manipulator

The robotic manipulator consists of a robotic arm body, a soft gripper body and 7 SCP actuators. The ball-and-socket joints composing the robotic arm body are 3D printed by polybutylene terephthalate (PBT) and the soft gripper body is 3D printed by polyurethane. SCP actuators are assembled to the two ball-and-socket joints and the gripper with pre-tension of 0.2 N. Then we integrated the arm and the soft gripper to build a robotic manipulator. The dimensions and workspace of the proposed robotic manipulator are listed in Table I. The control board is shown as Fig. 5. We used 4 serial 18650 Lithium ion batteries (maximum output: 14.8 V/ 5 A) and adjusted the voltage input using a voltage regular (LM2596S DC-DC). The voltage pulse was controlled using the electromagnetic relay (SRD-05VDC-SL-C). An Arduino UNO was used to collect data, control the relay and communicate with PC.

IV. EXPERIMENTS

As discussed in previous sections, the accumulation of Joule heating is the driving force for the contraction of the SCP. However, a direct method to measure the temperature is not available as the small size of SCP, which prohibits the use of an infrared thermometer or thermocouple [26]. Fortunately, SCP actuator could have an ideal linear displacement

TABLE I: PARAMETERS OF THE ROBOTIC MANIPULATOR

Parameters	Values
SCP Actuators Length for the Robotic Arm	105 mm
SCP Actuator Length for the Soft Gripper	55 mm
Maximum Angle Output for Each Ball Joint	14°
Power Supply for Maximum Angle Output	14 V, 5 A
Original Gripper Fingertip Distance	35 mm
Maximum Gripper Fingertip Distance Variation	30 mm
Power Supply for Maximum Gripper Fingertip Distance Variation	7 V, 3.01 A

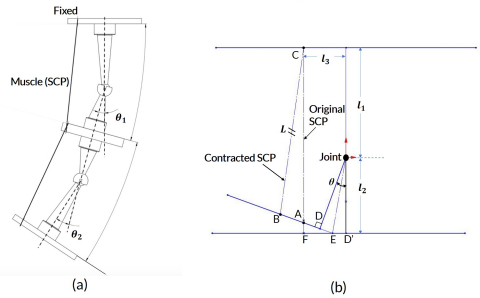

Fig. 6: Model for open loop control. (a) Geometric relation of the robotic arm. (b) Geometric relation of contracted SCP in a single joint.

output performance with applied electrical voltage under isometric conditions. Thus, we could build direct relationship between electric input and mechanical output based on the characteristics of the actuator, which means we could use a simple electro-mechanical open-loop control model to produce the desired displacement and force [27]. However, open-loop control is usually not accurate especially when there is disturbance in the working environment. Therefore, it's also necessary to design a closed-loop system to control the robotic manipulator. Open-loop and closed-loop control of SCP actuators are also reported in literature [13], however many parameters need to be tested and considered for the control. Moreover, the control in their study is aimed at a single actuator. Different from their research, the closed loop control in our study is aimed at a robotic module (joint), which is simple and easy to achieve.

A. Open-loop control of the robotic arm

A geometric relation between the displacement of the SCP actuators and the rotational angles is shown as Fig. 6. According to the relationship between the displacement of the SCP actuator and the applied voltage, we could get a direct relationship between the rotation angle of each joint θ and voltage input. To obtain the relationship, we have made some assumptions in this study:

1) Ball-and-socket joint rotates smoothly with negligible friction;

2) SCP Muscles keep tight and move smoothly through the fixed holes without friction and jerks;

3) Input displacement of SCP muscle is known previously for applied voltage using the linear model based on experimental measurements [28];

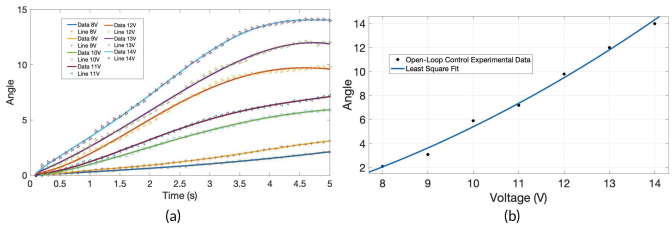

Fig. 7: Open-loop control result of the robotic manipulator's single joint. (a) Time domain angle change under various voltages. (b) Maximum angle output with respect to voltage.

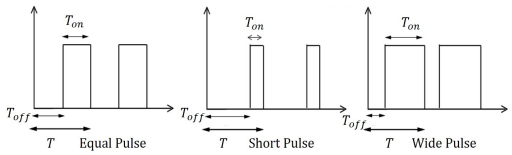

Fig. 8: Pulse control scheme.

4) The extending of unactuated muscles due to the contraction of actuated muscles does not affect the displacement of actuated muscle.

And from the Fig. 6(b), we can get the contracted SCP length in $\triangle ABC$:

$$AB = BD - AD = l_3 - \frac{l_3 - l_2 tan\frac{\theta}{2}}{cos\theta} + l_2 tan\frac{\theta}{2} \tag{1}$$

$$AC = l_1 + l_2 - (l_3 - l_2 tan\frac{\theta}{2}) tan\theta \tag{2}$$

$$cos\angle BAC = sin\theta \tag{3}$$

Using cosine theorem we can get:

$$BC^2 = AB^2 + AC^2 - 2 \times AB \times AC \times sin\theta \tag{4}$$

Since joint rotation angle θ is small in this study, approximation is made as: $sin\theta \approx \theta$. Substitute Eq. (4) equation with Eqs. (1)-(3), we can get the relationship between the length of contracted SCP (denoted as L) and angle θ as follows:

$$\theta = \alpha \times L^2 + \beta \tag{5}$$

where $\alpha = -\frac{1}{2l_1 l_3 + 2l_2 l_3}$, $\beta = \frac{(l_1+l_2)^2}{2l_1 l_3 + 2l_2 l_3}$.

Thus, we could control the robotic manipulator using open-loop control based on the relationship between θ and L given in Eq. (5). We used a GY 25 Tilt Mode to measure the angle and the input voltage increased from 8 V to 14 V with a 5s on. Fig. 7(a) shows the time domain angle changed for a single ball joint moving under various voltage input values. It is obvious that with larger voltage input, the angle output reach the steady value faster. And Fig. 7(b) exhibits a 2nd order relationship between the steady or maximum angle output and increased voltage, which is validated from the geometric relationship derivation. Thus, we could control the robotic manipulator with simple open-loop control.

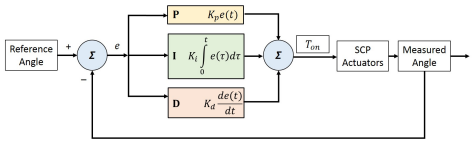

Fig. 9: Closed-loop control for joint angle of the arm using a feedback design.

B. Close-loop control of the robotic arm

From previous discussion, the relationship between joint angle output and voltage input is nonlinear, thus in order to get more accurate angle output, we need to use a feedback control system to control the SCP muscle based on the angle feedback. In this study, the measured joint angle from the GY 25 Tilt Mode is utilized to build the closed loop system.

The actuation of the SCP muscle is based on the Joule-heating, thus we could use an impulse voltage and modulate the width of the positive pulse to adjust the accumulation of Joule-heating. Fig. 8 shows the applied voltage pulse, here T period is 0.5 s.

Closed-loop control of angles is performed by closing the loop on the error between a reference angle and measured angle. Fig. 9 shows the closed-loop control design, according to the error, we used a proportional term K_p to amplify it, which could reduce the rise time, however, would have large overshoot. Thus, we used the addition of integral term K_i and derivative term K_d to reduce the overshoot and steady state error. Then map the output to the width of the positive pulse (T_{on}) from 0 to T.

Using a 10 V power supply, we were able to achieve the desired angle with a steady state with a mean error of 1.94%, as Fig. 10(a) shown. Here, the dotted lines indicate the target angle while the measured real angle data are fitted using a 7th order polynomial and shown as solid line. Fig. 10(b) shows that with a higher power supply, it could have faster response without large overshoot and could produce larger angle output (steady state mean error 1.73%).

According to Fig. 7 and Fig. 10, we can find that closed loop control can get a more accurate angle output (steady state mean error around 2% for closed loop control and 8% for open loop control). Then, closed loop control has a faster response (around 3 s response for 12-V power supply closed loop control and 5 s for open-loop control). For open loop control, achieving different angle needs provide various voltage, where closed loop control only needs a constant power supply. Closed loop control can also solve environmental noise, because of the feedback loop. The detailed comparison between closed loop control and open loop control is listed in Table II.

C. Characterization of the soft gripper

In this section, we also applied a square voltage to the SCP actuator. The contraction of the SCP leads to a shortening of the distance between the fingers. The base of the gripper was fixed and then we measured the distance between the fingertips. The experiment setup is showed in Fig. 11(a). The power-on time is 5 s and 10 s, and the power-off time is 40 s

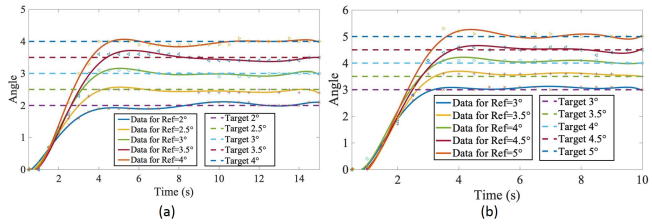

Fig. 10: Feedback control result. (a) With 10-V power supply. (b) With 12-V power supply.

TABLE II: THE COMPARISON BETWEEN CLOSED LOOP CONTROL AND OPEN LOOP CONTROL

Type of control	Steady state mean error	Response time	Power supply	Anti-interference
Closed loop control	2%	3 s	Constant voltage	Yes
Open loop control	8%	5 s	Various voltage	No

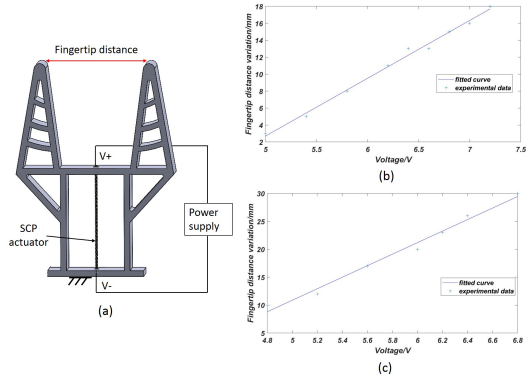

Fig. 11: Soft gripper characterization. (a) Experimental setup. (b) SCP actuator 5 s power on. (c) SCP actuator 10 s power on.

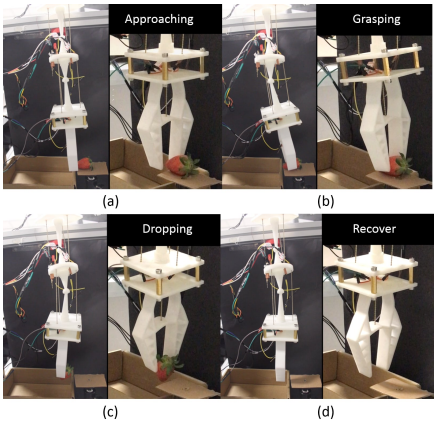

Fig. 12: The process of pick and drop a strawberry using the proposed robotic manipulator. (a) Approaching to the strawberry. (b) Grasping the object. (c) Dropping the object. (d) Recovering to original state.

and 50 s, respectively. The distance-to-voltage relationship is illustrated in Fig. 11(b) and Fig. 11(c), where we can see that the distance-to-voltage relationship presents a good linearity. Thus, we can simply get the desirable distance by adjusting the applied voltage input.

D. Grasping demonstration of the robotic manipulator

In this test, we integrate the ball-and-socket joint based robotic arm with a soft material gripper to build a compact robotic manipulator. The robotic manipulator is used to pick and place a strawberry from a platform to a paper box based on the angular feedback control, snap shots of the application demo are shown in Fig. 12. Firstly, the robotic arm is powered to approach the strawberry (Fig. 12(a)). Then, the soft gripper is power on to grasp the strawberry (Fig. 12(b)). Due to the soft material composing the gripper and the Fin Ray structure, the gripper can perform safe contact with the fragile object and adapt well to the object's shape passively. After grasping, the robotic arm moves to the designated position and SCP muscle in the soft gripper is powered off to drop the strawberry in the box (Fig. 12(c)). Lastly, robotic manipulator returns and recovers to its primary state (Fig. 12(d)) and a grasping task is completed. The grasping demonstration of the proposed robotic manipulator can also be seen in the video attachment of this paper.

V. CONCLUSIONS

Artificial muscles are attracting lots of academic attention recently [29-31] and they provide new alternatives for robotic actuation. In this study, we have presented a novel robotic manipulator powered by the high-performance SCP artificial muscles. The manipulator is composed by a robotic arm and an end effector. The robotic arm design takes inspiration from musculoskeletal system. A simple open-loop control of the bio-inspired arm is built, which is based on the geometric relationship derivation. Furthermore, a closed-loop control is designed to provide more accurate and steady angle output. These controls do not rely on complicated model with experimentally tested parameters, yet are proved to be effective. At last, we integrate the ball-and-socket joint based robotic arm with a Fin Ray Effect inspired soft gripper as an end effector to build a whole robotic manipulator using SCP muscles as actuators. For demonstration, this robotic manipulator is utilized to pick and place a fragile fruit from a platform to a box based on the angle feedback control.

Both the bio-inspired robotic arm and the soft griper are actuated by SCP muscles thus requires no extra motors, making the whole robotic manipulator compact. The material we used to 3D print the arm is PBT, which is $11.54 per kilogram. And for polyurethane, which used in soft gripper is $28.26 per kilogram. Nylon fishing line used to fabricate SCP is $0.3 per meter. Thus, the total cost of our manipulator is $3.5, which is extremely low. Therefore, the whole robotic manipulator in this study is low-cost.

In future, we can change the arrangement of the SCP muscles in the robotic arm to change the degrees of freedom of the manipulator. More ball joints will also be cascaded to construct a hyper-redundant robotic arm (as elephant truck type) [32]. In addition, pressure sensor will also be integrated to the soft gripper to realize close-loop contact force control.

REFERENCES

[1] S. Ikemoto, Y. Kimoto, and K. Hosoda, "Shoulder complex linkage mechanism for humanlike musculoskeletal robot arms," *Bioinspir. Biomim.*, vol. 10, no. 6, p.066009, 2015.

[2] Z. Xu and E. Todorov, "Design of a highly biomimetic anthropomorphic robotic hand towards artificial limb regeneration," in *Proc. IEEE Int. Conf. Robot. Autom.*, 2016, pp. 3485-3492.

[3] C. Richter et al., "Musculoskeletal robots: scalability in neural control," *IEEE Robot. Autom. Mag.*, vol. 23, no. 4, pp.128-137, 2016.

[4] R. Bogue, "Artificial muscles and soft gripping: a review of technologies and applications," *Ind. Robot*, vol. 39, no. 6, pp. 535-540, 2012.

[5] J. Mintenbeck, R. Estaña, and H. Woern, "Design of a modular, flexible instrument with integrated DC-motors for minimal invasive robotic surgery," in *Proc. IEEE/ASME Int. Conf. Adv. Intel. Mechatron.*,, 2013, pp. 1249-1254.

[6] C. B. Yigit and P. Boyraz, "Design and modelling of a cable-driven parallel-series hybrid variable stiffness joint mechanism for robotics," *Mech. Sci.*, vol. 8, no. 1, pp. 65-77, 2017.

[7] J. Zhang et al., "Robotic Artificial Muscles: Current Progress and Future Perspectives," *IEEE Trans. Robot.*, vol. 35, no. 3, pp. 761–781, 2019.

[8] P. Polygerinos et al., "Soft robotics: Review of fluid-driven intrinsically soft devices; manufacturing, sensing, control, and applications in human-robot interaction," *Adv. Eng. Mater.*, vol. 19, no. 12, p.1700016, 2017.

[9] H. Rodrigue et al., "An overview of shape memory alloy-coupled actuators and robots," *Soft Robot.*, vol. 4, no. 1, pp. 3-15, 2017.

[10] F. Chen, M. Y. Wang, J. Zhu, and Y. F. Zhang, "Interactions between dielectric elastomer actuators and soft bodies," *Soft Robot.*, vol. 3, no. 4, pp. 161-169, 2016.

[11] K. Jung, J. Nam, and H. Choi, "Investigations on actuation characteristics of IPMC artificial muscle actuator," *Sensors Actuators A, Phys.*, vol. 107, no. 2, pp. 183-192, 2003.

[12] C. S. Haines et al., "Artificial muscles from fishing line and sewing thread," *Science*, vol. 343, no. 6173, pp. 868–872, 2014.

[13] M. C. Yip and G. Niemeyer, "On the control and properties of supercoiled polymer artificial muscles," *IEEE Trans. Robot.*, vol. 33, no. 3, pp. 689–699, 2017.

[14] L. Wu et al., "Compact and low-cost humanoid hand powered by nylon artificial muscles," *Bioinspir. Biomim.*, vol. 12, no. 2, p. 026004, 2017.

[15] L. Sutton et al., "Design of an assistive wrist orthosis using conductive nylon actuators," in *Proc. IEEE Int. Conf. Biomed. Robot. Biomech.*, 2016, pp. 1074–1079.

[16] Y. Yang et al., "A Low-cost Inchworm-inspired Soft Robot Driven by Supercoiled Polymer Artificial Muscle," in *Proc. IEEE Int. Conf. Soft Robot.*, 2019, pp. 161-166.

[17] J. Sun, B. Pawlowski, and J. Zhao, "Embedded and Controllable Shape Morphing with Twisted-and-Coiled Actuators," in *Proc. IEEE/RSJ Int. Conf. Intell. Robot. Syst.*, 2018, pp. 5912-5917.

[18] B. Pawlowski et al., "Modeling of Soft Robots Actuated by Twisted-and-Coiled Actuators," *IEEE/ASME Trans. Mechatron.*, vol. 24, no. 1, pp. 5-15, 2019.

[19] S. M. Mirvakili and I. W. Hunter, "Artificial muscles: Mechanisms, applications, and challenges," *Adv. Mater.*, vol. 30, no. 6, p.1704407, 2018.

[20] L. Wu, I. Chauhan, and Y. Tadesse, "A Novel Soft Actuator for the Musculoskeletal System," *Adv. Mater. Technol.*, vol. 3, no. 5, p.1700359, 2018.

[21] L. Kniese, "Load carrying element with flexible outer skin," European Patent, EP1040999A2, 1999.

[22] W. Crooks et al., "Fin ray effect inspired soft robotic gripper: from the robosoft grand challenge toward optimization," *Front. Robot. AI*, vol. 3, p.70, 2016.

[23] C. I. Basson, G. Bright, and A.J. Walker, "Testing flexible grippers for geometric and surface grasping conformity in reconfigurable assembly systems," *S. Afr. J. Ind. Eng.*, vol. 29, no. 1, pp.128-142, 2018.

[24] J. Zhang et al., "Modeling and inverse compensation of hysteresis in supercoiled polymer artificial muscles," *IEEE Robot. Autom. Lett.*, vol. , no. 2, pp. 773-780, 2017.

[25] F. Karami and Y. Tadesse, "Modeling of twisted and coiled polymer (TCP) muscle based on phenomenological approach," *Smart Mater. Struct.*, vol. 26, no. 12, p.125010, 2017.

[26] M. Suzuki and N. Kamamichi, "Displacement control of an antagonistic-type twisted and coiled polymer actuator," *Smart Mater. Struct.*, vol. 27, no. 3, p.035003, 2018.

[27] T. A. Luong et al., "Nonlinear Tracking Control of a Conductive Supercoiled Polymer Actuator," *Soft Robot.*, vol. 5, no. 2, pp. 190-203, 2018.

[28] Y. Yang et al., "A Novel Variable Stiffness Actuator Based on Pneumatic Actuation and Supercoiled Polymer Artificial Muscles," in *Proc. IEEE Int. Conf. Robot. Autom.*, 2019, pp. 3983-3989.

[29] M. Kanik et al., "Strain-programmable fiber-based artificial muscle," *Science*, vol. 365, no. 6449, pp. 145-150, 2019.

[30] J. Mu et al., "Sheath-run artificial muscles," *Science*, vol. 365, no. 6449, pp. 150-155, 2019.

[31] J. Yuan et al., "Shape memory nanocomposite fibers for untethered high-energy microengines," *Science*, vol. 365, no. 6449, pp. 155-158, 2019.

[32] Y. Yang et al., "3D printing of variable stiffness hyper-redundant robotic arm," in *Proc. IEEE Int. Conf. Robot. Autom.*, 2016, pp. 3871-3877.